

## Supporting information

### Poly (Triethylene Glycol Methyl Ether Methacrylate) Hydrogel as Carriers of Phosphotungstic Acid for Acid Catalytic Reaction in Water

JunJie Zhu<sup>a</sup>, Takehiko Gotoh<sup>\*a</sup>, Satoshi Nakai<sup>a</sup>, Nao Tsunoji<sup>b</sup> and Masahiro Sadakane<sup>\*\*b</sup>

<sup>a</sup> Department of Chemical Engineering, Graduate School of Advanced Science and Engineering, Hiroshima University, 1-4-1 Kagamiyama, Higashi-Hiroshima, 739-8527, Japan

<sup>b</sup> Department of Applied Chemistry, Graduate School of Advanced Science and Engineering, Hiroshima University, 1-4-1 Kagamiyama, Higashi-Hiroshima, 739-8527, Japan.

\*tgoto@hiroshima-u.ac.jp, \*\*sadakane09@hiroshima-u.ac.jp

#### Contents:

S1	Experimental Details	
□	Materials	2
□	Synthesis of H <sub>3</sub> PW <sub>12</sub> O <sub>40</sub> -poly-TEGMA composite	2
□	Leaching test	2
□	Characterizations	2
□	Catalyst testing	3
S2	Preparation and characterization of H <sub>3</sub> PW <sub>12</sub> O <sub>40</sub> -poly-TEGMA composite	
□	Photo of TEGMA monomer solutions containing H <sub>3</sub> PW <sub>12</sub> O <sub>40</sub> (Fig. S1(a)).....	4
□	Absorbances at 380.5 nm of TEGMA monomer solutions. (Fig. S1(b)) .....	4
□	Refractive index of mixed solution and composite. (Fig. S2) .....	5
□	Photo of plates of H <sub>3</sub> PW <sub>12</sub> O <sub>40</sub> -poly-TEGMA composites. (Fig. S3) .....	5
□	FT-IR spectra of poly-TEGMA hydrogel. (Fig. S4) .....	6
□	Ball-and-stick representation of H <sub>3</sub> PW <sub>12</sub> O <sub>40</sub> . (Fig. S5) .....	7
□	XRD patterns of poly-TEGMA hydrogel. (Fig. S6) .....	8
□	SEM patterns of poly-TEGMA hydrogel. (Fig. S7) .....	9
□	Swelling behavior of H <sub>3</sub> PW <sub>12</sub> O <sub>40</sub> -poly-TEGMA-composites. (Fig. S8(a)) .....	10
□	Swelling volumes of H <sub>3</sub> PW <sub>12</sub> O <sub>40</sub> composites. (Fig. S8 (b)) .....	10
□	Conversion of ethyl acetate with different content ratio composite. (Table. S1) ...	11

#### S1: Experimental Details

**Materials:** Monomer: TEGMA (triethylene glycol methyl ether methacrylate) was obtained from

Hitach Chemicals Co., Ltd. Crosslinker: TEGDMA (triethylene glycol dimethacrylate) was obtained from Tokyo Chemical Industry Co., Ltd. Initiator: AIBN (2,2'-azobis(isobutyronitrile)) was obtained from Nacalai Tesque, INC. The Keggin-type phosphotungstic acid,  $\text{H}_3\text{PW}_{12}\text{O}_{40}$ , was obtained from Nippon Inorganic Colour & Chemical Co., Ltd. All chemicals were of reagent grade and were used as supplied. The water used in all the experiments was distilled.

**Synthesis of  $\text{H}_3\text{PW}_{12}\text{O}_{40}$ -poly-TEGMA composite:** All the  $\text{H}_3\text{PW}_{12}\text{O}_{40}$ -poly-TEGMA composites were synthesized via the free-radical polymerization method with initial amounts of the  $\text{H}_3\text{PW}_{12}\text{O}_{40}$  additive of 10 wt%, 20 wt%, 40 wt%, 60 wt%, and 80 wt%. Three grams of TEGMA were mixed with 0.1851 g of TEGDMA, and the calculated amounts of  $\text{H}_3\text{PW}_{12}\text{O}_{40}$  were added to the solution and stirred for 2 h at room temperature. The obtained solution was homogenized by stirring and then purged with nitrogen gas for 1 h to remove dissolved oxygen. Then, 0.01 g of AIBN was added to the solution and stirred for 2 min. The obtained mixture was then injected into the gel-plate formation kit (AE-6401 1-mm Dual Mini Gel Cast, ATTO Corp.). The reaction was conducted at 45 °C for 24 h. After the composites were synthesized, they were cut into 10 mm × 10 mm × 1 mm plates. Finally, the  $\text{H}_3\text{PW}_{12}\text{O}_{40}$ -poly-TEGMA composites were air dried at room temperature for 1 day, followed by further drying at 50 °C for 1 day in a drying oven.

**Leaching test:** One gram of the  $\text{H}_3\text{PW}_{12}\text{O}_{40}$ -poly-TEGMA composite was placed into a tea pack, which was then immersed in 3L of distilled water and stirred for 24 h at 298 K. The composite was then removed from the solution and dried at 323 K. This procedure was repeated several times. The samples (approx. 20 mg) were placed into a TGA-50 (SHIMADZU) thermogravimetric (TG) analyzer and heated in a flow of air at 20 K min<sup>-1</sup> from room temperature to 873 K, which was maintained for 20 mins. The concentration of  $\text{H}_3\text{PW}_{12}\text{O}_{40}$  in the composite was calculated from the weight losses.

**Characterizations:** The Fourier-transform infrared (FT-IR) spectra were recorded in the range of 600–2500 cm<sup>-1</sup> on a NICOLET 6700 FT-IR spectrometer (Thermo Fisher Scientific). Powder X-ray diffraction (XRD) patterns were measured with a MiniFlex600 (RIGAKU) diffractometer using Cu K $\alpha$  radiation at ambient temperature. Scanning electron microscopy (SEM) and energy-dispersive X-ray spectroscopy (EDX) analyses were performed using an S-5200 (HITACHI High-Technologies) field-emission SEM at acceleration voltages of 3.0 kV and 15.0 kV, respectively. The samples for the SEM analysis were dusted onto adhesive conductive carbon paper attached to a brass sample mount. TG analysis was performed using a TGA-50 (SHIMADZU) thermogravimetric analyzer. The proton nuclear magnetic resonance (<sup>1</sup>HNMR) spectra were recorded on a Varian 500 spectrometer (H resonance frequency: 499.939 MHz). These spectra were referenced to the internal HOD (4.659 ppm). The refractive index was measured with an Abbe refractometer DR- A1 (ATAGO).

**Catalyst testing:** The acid catalytic activity of  $\text{H}_3\text{PW}_{12}\text{O}_{40}$  in the polymer composites was determined during the hydrolysis of ethyl acetate by measuring the <sup>1</sup>HNMR spectra.<sup>33</sup> In a typical experiment, 0.05 g of the composite was added to 3 ml of ethyl acetate D<sub>2</sub>O solution (150 mg in

3mL), and the reaction mixture was maintained at 298 K while stirring. After the reaction, the mixture was separated using a polyethersulfone membrane filter (0.22  $\mu\text{m}$ ), and the solution was injected into an NMR test tube for  $^1\text{H}$ NMR analysis of the conversion rate and yield. In the  $^1\text{H}$ NMR spectra, peaks were observed to correspond to ethyl acetate, ethyl alcohol, and acetic acid, with no other peaks were observed. Therefore, we assumed that the selectivity of this hydrolysis reaction was 100%. As the peaks of methylene ( $\text{CH}_2\text{O}$ ) for ethyl acetate (4.03) and ethyl alcohol (3.52) were well separated, the conversion of ethyl acetate was calculated based on the integration ratio of these two peaks as follows:

Conversion = (integration of  $\text{CH}_2\text{O}$  of ethyl alcohol) / (integration of  $\text{CH}_2\text{O}$  of ethyl acetate + integration of  $\text{CH}_2\text{O}$  of ethyl alcohol).

$^1\text{H}$ NMR of ethyl acetate in  $\text{D}_2\text{O}$  (HOD peak at 4.75 ppm): 1.13 ppm ( $\text{CH}_3\text{CH}_2$ , triplet, 3H), 1.97 ppm ( $\text{CH}_3\text{CO}$ , singlet, 3H), 4.03 ppm ( $\text{CH}_2\text{O}$ , quartet, 2H)

$^1\text{H}$ NMR of ethyl alcohol in  $\text{D}_2\text{O}$  (HOD peak at 4.75 ppm): 1.06 ppm ( $\text{CH}_3\text{CH}_2$ , triplet, 3H), 3.52 ppm ( $\text{CH}_2\text{O}$ , quartet, 2H)

$^1\text{H}$ NMR of acetic acid in  $\text{D}_2\text{O}$  (HOD peak at 4.75 ppm): 1.97 ppm ( $\text{CH}_3\text{CO}$ , singlet, 3H)

**S2: Preparation and characterization of  $\text{H}_3\text{PW}_{12}\text{O}_{40}$ -poly-TEGMA composite**

At 298 K, the  $\text{H}_3\text{PW}_{12}\text{O}_{40}$  solid can be fully dissolved in the TEGMA monomer at a high concentration (approx. 80 wt%) to form a clear and stable solution. The color of the solution gradually turned light yellow with increases in the  $\text{H}_3\text{PW}_{12}\text{O}_{40}$  concentration (Fig. S1(a)). Similarly, the dissolving of  $\text{H}_4\text{SiW}_{12}\text{O}_{40}$  in acrylate ester molecules has been reported.<sup>32</sup> The refractive index of the solution also increased with the addition of  $\text{H}_3\text{PW}_{12}\text{O}_{40}$  (Fig. 1S2, black balls). Lastly, clear plate composites were produced by free-radical polymerization using AIBN as an initiator and the TEGMA monomer with TEGDMA as a crosslinker (Fig. S23).

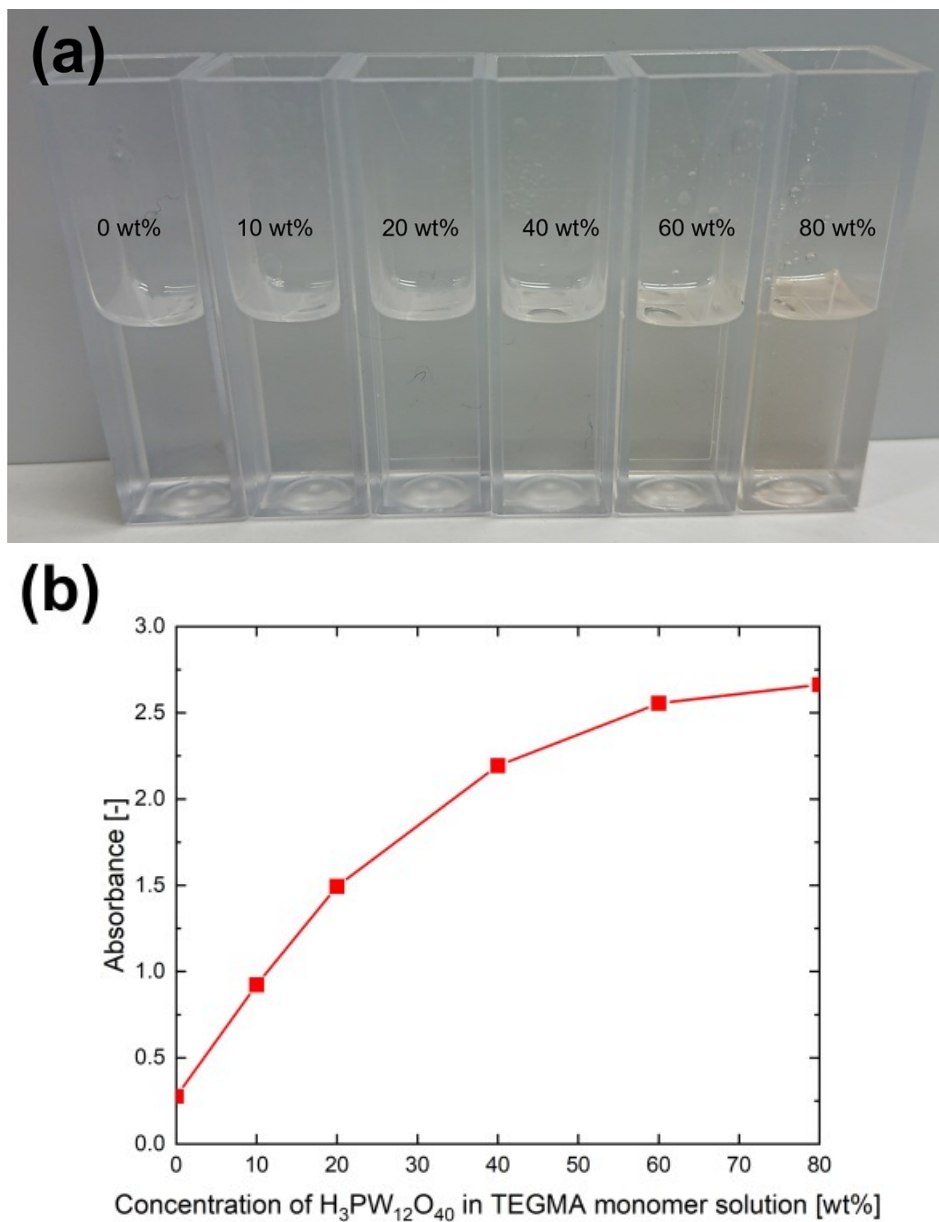


Fig. S1 Photo of TEGMA monomer solutions containing 0-wt%, 10-wt%, 20-wt%, 40-wt%, 60-wt%, and 80-wt%  $\text{H}_3\text{PW}_{12}\text{O}_{40}$  (a), absorbances at 380.5 nm of TEGMA monomer solutions containing 0-wt%, 10-wt%, 20-wt%, 40-wt%, 60-wt%, and 80-wt%  $\text{H}_3\text{PW}_{12}\text{O}_{40}$  (b).

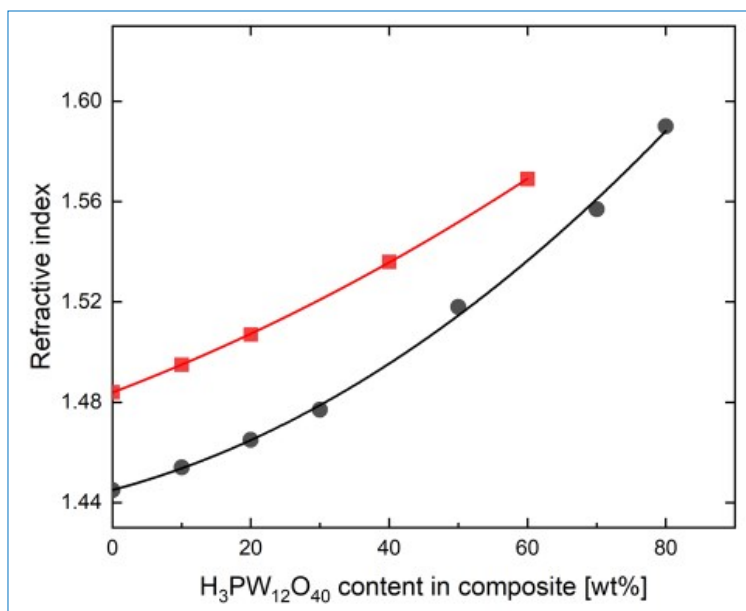


Fig. S2 Refractive index of the H<sub>3</sub>PW<sub>12</sub>O<sub>40</sub>-TEGMA monomer mixed solution (black balls) and H<sub>3</sub>PW<sub>12</sub>O<sub>40</sub>-poly-TEGMA composites (red squares) against H<sub>3</sub>PW<sub>12</sub>O<sub>40</sub> content (wt %).

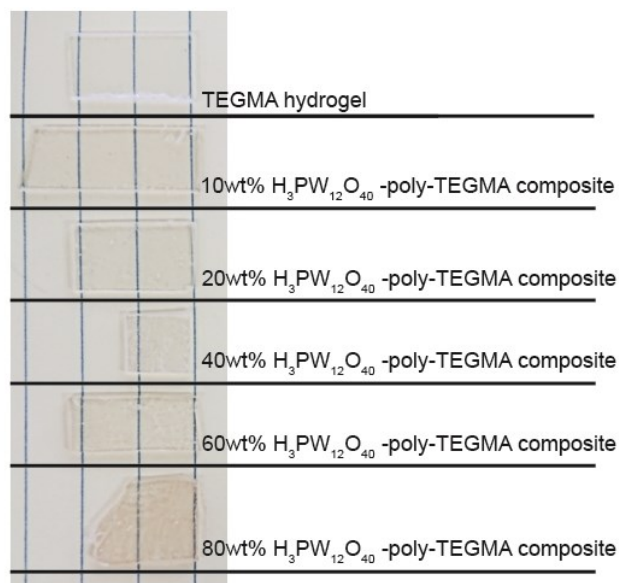


Fig. S3 Photo of plates of poly-TEGMA hydrogel and H<sub>3</sub>PW<sub>12</sub>O<sub>40</sub>-poly-TEGMA composites with 10 wt%, 20 wt%, 40 wt%, 60 wt%, and 80 wt% of H<sub>3</sub>PW<sub>12</sub>O<sub>40</sub>.

Figure S4 shows the FT-IR spectra of the poly-TEGMA hydrogel, pure  $\text{H}_3\text{PW}_{12}\text{O}_{40}$ , and  $\text{H}_3\text{PW}_{12}\text{O}_{40}$ -poly-TEGMA composites. For the IR spectrum of pure  $\text{H}_3\text{PW}_{12}\text{O}_{40}$ , the absorption bands at  $1081\text{ cm}^{-1}$ ,  $978\text{ cm}^{-1}$ ,  $896\text{ cm}^{-1}$ , and  $802\text{ cm}^{-1}$  are characteristic of the absorptions of the  $\text{P-O}_a$  bond and the three  $\text{W-O}$  bonds ( $\text{O}_d$ , terminal oxygen to W;  $\text{O}_b$ , corner-sharing oxygen;  $\text{O}_c$ , edge sharing oxygen), respectively (Fig. S5).<sup>29</sup> The IR spectra of the 10–80-wt%  $\text{H}_3\text{PW}_{12}\text{O}_{40}$ -poly-TEGMA composite show the characteristic bands of  $\text{H}_3\text{PW}_{12}\text{O}_{40}$ , which indicates the structural integrity of  $\text{H}_3\text{PW}_{12}\text{O}_{40}$  in the composites. The intensities of these bands strengthen with increases in the  $\text{H}_3\text{PW}_{12}\text{O}_{40}$  content. Interestingly, the absorption peak at  $802\text{ cm}^{-1}$ , which corresponds to the vibration of  $\text{W-O}_c$  in  $\text{H}_3\text{PW}_{12}\text{O}_{40}$ , becomes sharper and shifts to  $820\text{ cm}^{-1}$  (for 40 wt%  $\text{H}_3\text{PW}_{12}\text{O}_{40}$ -poly-TEGMA composite), which implies hydrogen bonding interaction between  $\text{H}_3\text{PW}_{12}\text{O}_{40}$  and TEGMA. A similar shape change and wavelength shift of the band at  $802\text{ cm}^{-1}$  was observed when  $\text{H}_3\text{PW}_{12}\text{O}_{40}$  was mixed with poly(ethylene glycol).<sup>29</sup> This suggests that the bridging oxo ligand,  $\text{O}_c$ , has a comparatively higher negative charge and thus behaves as a hydrogen bonding acceptor group. The oxygens in  $\text{H}_3\text{PW}_{12}\text{O}_{40}$  can form hydrogen bonds with the ether groups of TEGMA, thereby contributing to the high solubility of  $\text{H}_3\text{PW}_{12}\text{O}_{40}$  in the TEGMA monomer.<sup>29,34</sup>

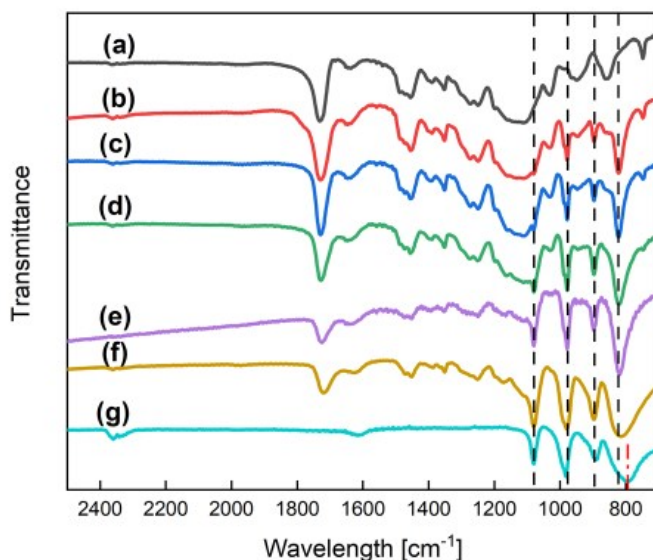


Fig. S4 FT-IR spectra of poly-TEGMA hydrogel (a), 10-wt%  $\text{H}_3\text{PW}_{12}\text{O}_{40}$ -poly-TEGMA composite (b), 20-wt%  $\text{H}_3\text{PW}_{12}\text{O}_{40}$ -poly-TEGMA composite (c), 40-wt%  $\text{H}_3\text{PW}_{12}\text{O}_{40}$ -poly-TEGMA composite (d), 60-wt%  $\text{H}_3\text{PW}_{12}\text{O}_{40}$ -poly-TEGMA composite (e), 80-wt%  $\text{H}_3\text{PW}_{12}\text{O}_{40}$ -poly-TEGMA composite (f) and  $\text{H}_3\text{PW}_{12}\text{O}_{40}$  (g).

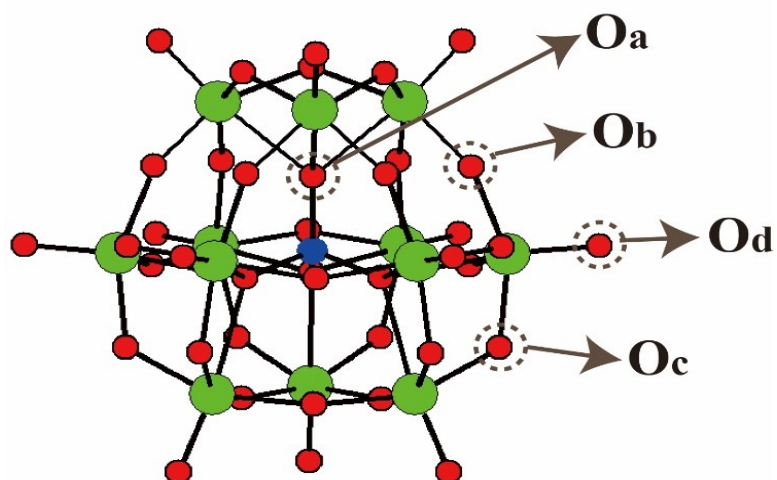


Fig. S5 Ball-and-stick representation of  $\text{H}_3\text{PW}_{12}\text{O}_{40}$ .  $\text{O}_a$ ,  $\text{O}_b$ ,  $\text{O}_c$ , and  $\text{O}_d$  represent the O bond to P, corner-sharing oxygen between Ws, edge-shared oxygen between Ws, and terminal oxygen on W, respectively.

Figure S6 shows the XRD patterns of the poly-TEGMA hydrogel, pure  $\text{H}_3\text{PW}_{12}\text{O}_{40}$ , and  $\text{H}_3\text{PW}_{12}\text{O}_{40}$ -poly-TEGMA composites. Only broad diffraction peaks were observed in the 10–80-wt%  $\text{H}_3\text{PW}_{12}\text{O}_{40}$ -poly-TEGMA composites, and no diffraction peak was assignable to the crystalline  $\text{H}_3\text{PW}_{12}\text{O}_{40}$  species, which indicates that the  $\text{H}_3\text{PW}_{12}\text{O}_{40}$ -poly-TEGMA composites were amorphous. It can be inferred that the  $\text{H}_3\text{PW}_{12}\text{O}_{40}$  molecules were well dispersed in the poly-TEGMA carriers.

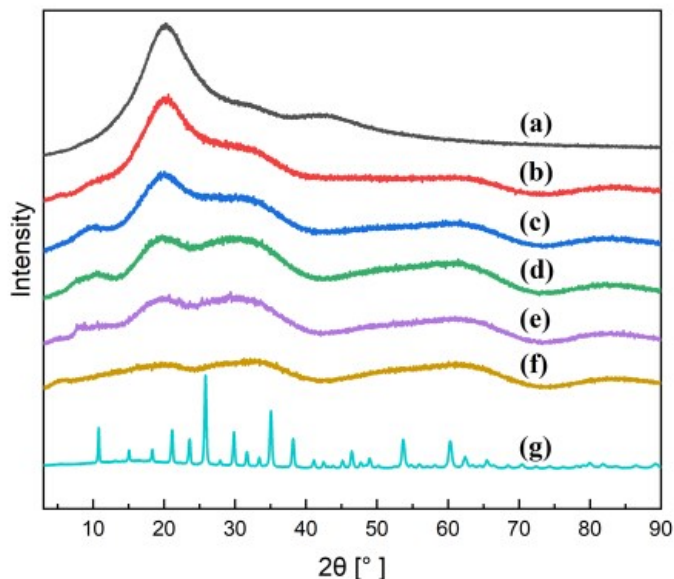


Fig. S6 XRD patterns of poly-TEGMA hydrogel (a), 10-wt%  $\text{H}_3\text{PW}_{12}\text{O}_{40}$ -poly-TEGMA composite (b), 20-wt%  $\text{H}_3\text{PW}_{12}\text{O}_{40}$ -poly-TEGMA composite (c), 40-wt%  $\text{H}_3\text{PW}_{12}\text{O}_{40}$ -poly-TEGMA composite (d), 60-wt%  $\text{H}_3\text{PW}_{12}\text{O}_{40}$ -poly-TEGMA composite (e), 80-wt%  $\text{H}_3\text{PW}_{12}\text{O}_{40}$ -poly-TEGMA composite (f) and  $\text{H}_3\text{PW}_{12}\text{O}_{40}$  (g).



Figure S7 shows SEM images of the poly-TEGMA hydrogel, 40-wt%  $\text{H}_3\text{PW}_{12}\text{O}_{40}$ -poly-TEGMA composite, and 80-wt%  $\text{H}_3\text{PW}_{12}\text{O}_{40}$ -poly-TEGMA composite. We can see that the poly-TEGMA hydrogel and 40-wt%  $\text{H}_3\text{PW}_{12}\text{O}_{40}$ -poly-TEGMA composite have relatively flat surfaces and similar surface states. When the  $\text{H}_3\text{PW}_{12}\text{O}_{40}$  loading concentration exceeds 80 wt%, many pocket-shaped cavities can be observed on the surface. Combined with the results of the leaching test, this suggests that the change in the surface state of the composite was related to the  $\text{H}_3\text{PW}_{12}\text{O}_{40}$  loading concentration. We can conclude that when the loading concentration of  $\text{H}_3\text{PW}_{12}\text{O}_{40}$  in the poly-TEGMA hydrogel reaches its limit, the surface morphology of the composite will change.

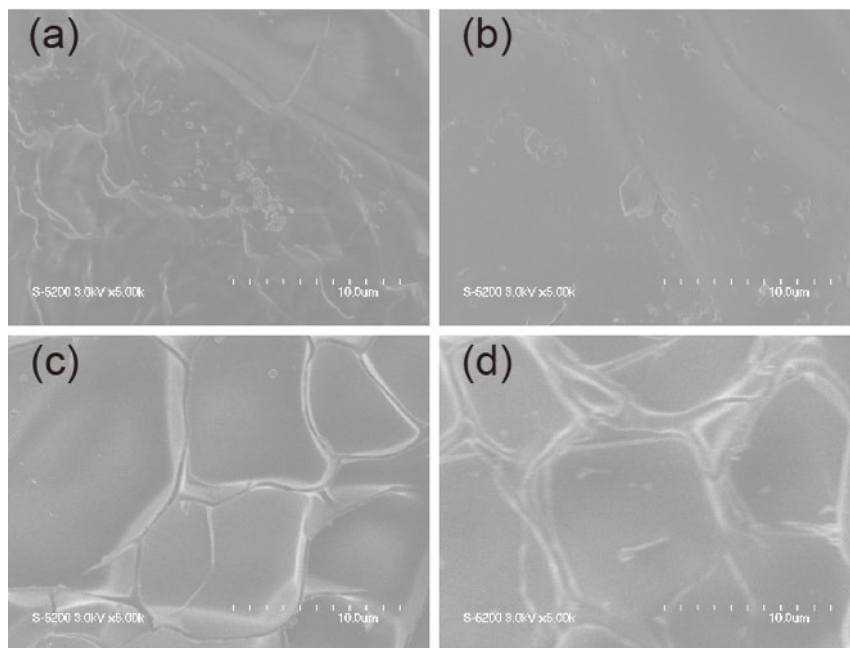


Fig. S7 SEM patterns of poly-TEGMA hydrogel (a), 40-wt%  $\text{H}_3\text{PW}_{12}\text{O}_{40}$ -poly-TEGMA composite (b), and 80-wt%  $\text{H}_3\text{PW}_{12}\text{O}_{40}$ -poly-TEGMA composites (c, d)

Figure S8(a) shows the swelling behavior of composites with different  $\text{H}_3\text{PW}_{12}\text{O}_{40}$  loading amounts, and Fig. S8(b) shows the calculated volume swelling rates. The volume of all the composites increases and the plate structure of the 80-wt%  $\text{H}_3\text{PW}_{12}\text{O}_{40}$ /TEGMA composite was broken (Fig. S8(a)). The poly-TEGMA composites swelled even in the presence of  $\text{H}_3\text{PW}_{12}\text{O}_{40}$ , with a volume swelling rate of about 3–4 (Fig. S7(b)). This swelling behavior may facilitate the composite's absorption of the reactant from the solution and the completion of the catalytic reaction with the catalyst in the composite.

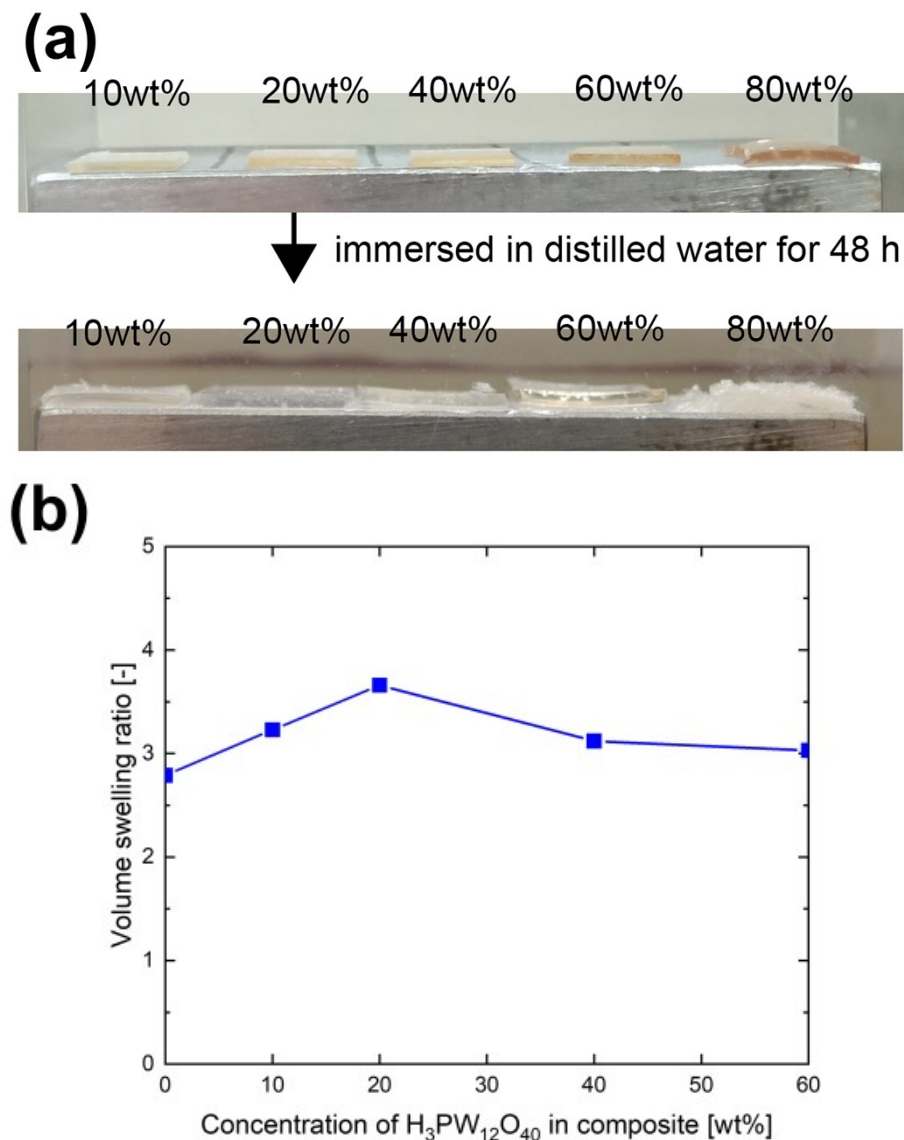


Fig. S8 Photos of swelling behavior of 10-wt%, 20-wt%, 40-wt%, 60-wt%, and 80-wt%  $\text{H}_3\text{PW}_{12}\text{O}_{40}$ -poly-TEGMA-composites in distilled water (a), swelling volumes of 10-wt%, 20-wt%, 40-wt%, 60-wt%, and 80-wt%  $\text{H}_3\text{PW}_{12}\text{O}_{40}$  composites (b).

Table. S1 shows the conversion of ethyl acetate after 72-hour with 0-wt%, 10-wt%, 20wt% and 40-wt%  $\text{H}_3\text{PW}_{12}\text{O}_{40}$ -poly-TEMGA composites. It shows higher the  $\text{H}_3\text{PW}_{12}\text{O}_{40}$  contents lead to higher catalytic activity.

$\text{H}_3\text{PW}_{12}\text{O}_{40}$ content	0-wt%	10-wt%	20-wt%	40-wt%
AcOEt hydrolysis rate	0.49%	4.13%	26.78%	36.91%

Table. S1 Conversion of ethyl acetate after 72-hour with 0-wt%, 10-wt%, 20wt% and 40-wt%  $\text{H}_3\text{PW}_{12}\text{O}_{40}$ -poly-TEMGA composites.